

Optical Reflectivity and Absorption Measurements of Sodium C222 Sodide

STEPHAN JAENICKE,* MARGARET K. FABER,†
AND JAMES L. DYE‡

*Department of Chemistry, Michigan State University,
East Lansing, Michigan 48824*

AND W. P. PRATT, JR.

*Department of Physics and Astronomy, Michigan State University,
East Lansing, Michigan 48824*

Received August 25, 1986

The reflectivity at normal incidence of single crystals of $\text{Na}^+\text{C}_{222} \cdot \text{Na}^-$ was measured from 350 to 2500 nm in a microreflectivity apparatus. The reflectivity spectrum shows a single peak at 630 ± 10 nm (1.97 eV) with a peak reflectivity of up to 60%. No rise in the reflectivity was found toward longer wavelengths. This absence of a plasma edge confirms that the concentration of conduction electrons is smaller than $1.8 \times 10^{20}/\text{cm}^3$ as expected from the low electrical conductivity of this sodide. The absorption spectrum of thin solid films of $\text{Na}^+\text{C}_{222} \cdot \text{Na}^-$, formed by vapor deposition, was measured *in situ* in a vacuum evaporator. The absorption peak was at 650 ± 10 nm (1.91 eV), with a full-width at half-maximum of 0.37 eV. The reflectivity and absorption data were used together to estimate the indices of refraction and absorption and the components of the complex dielectric constant as a function of wavelength. © 1987 Academic Press, Inc.

Introduction

Since the isolation of the first crystalline salt of an alkali metal anion (alkalide) in 1974 (1, 2), we have prepared and characterized (3-5) over 30 crystalline salts in which the anion is Na^- , K^- , Rb^- , or Cs^- . A characteristic feature of these salts is an intense absorption band, presumably arising

from an $ns \rightarrow np$ transition of the anion (4). Because it was necessary to use thin polycrystalline films prepared by solvent evaporation in previous studies, the transmission spectra (6-8) could not yield quantitative information about absorption coefficients or band shapes.

A great deal of information is now available for the "parent" compound sodium-cryptand(2.2.2)-sodide, $\text{Na}^+\text{C}_{222} \cdot \text{Na}^-$. Its crystal structure (2), thermodynamics of formation from sodium metal and cryptand (9), NMR spectrum (10-12), photoelectron spectrum (13), powder and single crystal conductivity (4, 14, 15), and absorption

* Present address: Fritz-Haber Institut der Max Planck Gesellschaft, Faradayweg 4-6, D-1000 Berlin 33, West Germany.

† Present address: Corning Glass Works, Sullivan Park DV-01-9, Corning, NY 14831.

‡ To whom correspondence should be addressed.

spectrum (6, 16) have been measured. The latter has been determined for films produced by both rapid solvent evaporation (6) and direct codeposition of Na and C222 from the vapor (16).

Recently an Ultek high-vacuum evaporator has been modified to grow thin solid films of alkaliides by physical vapor deposition. The thickness and stoichiometry of films were monitored so that quantitative and semiquantitative data could be obtained. This paper describes the measurement and interpretation of both the reflectivity at normal incidence of single crystals of $\text{Na}^+\text{C222} \cdot \text{Na}^-$ and the transmittance of thin vapor-deposited films of $\text{Na}^+\text{C222} \cdot \text{Na}^-$. These results were combined to determine the optical properties of this compound.

The optical behavior of an optically isotropic solid is completely determined by the frequency dependence of the complex index of refraction $N = n + ik$, in which n is the index of refraction and k is the index of absorption. The latter is connected to the absorption coefficient, α , by $\alpha = 4\pi k/\lambda$. The reflection coefficient, R_{12} , is given by

$$R_{12} = \frac{(n - 1)^2 + k^2}{(n + 1)^2 + k^2}. \quad (1)$$

Alternatively, one can formulate the complex dielectric function $\epsilon = \epsilon_1 + i\epsilon_2$. The two expressions are related by $N = \sqrt{\epsilon}$.

In order to determine the optical constants at a particular frequency it is necessary to make two measurements. If sufficiently transparent samples with parallel faces can be prepared, measurement of the transmission, T ,

$$T = \frac{(1 - R_{12})^2 \exp[-ad]}{1 - R_{12}^2 \exp[-2ad]}. \quad (2)$$

at two different thicknesses, or measurement of transmission and reflectivity, R ,

$$R = R_{12}[1 + T \exp(-ad)], \quad (3)$$

yields the necessary information. For an opaque sample, $R = R_{12}$.

In many cases, the absorption coefficient becomes so large that even the thinnest single crystal samples are opaque. Thin film techniques can provide information about the absorption coefficient, but they are not without problems. With a sample thickness or crystallite sizes comparable to the wavelength of the light, interference effects can become important. Thermally evaporated films or films produced by solvent evaporation are also generally less ordered than single crystals and may have voids between individual crystals which, especially at high optical densities, can seriously distort the observed absorption spectrum.

When the crystals are too opaque, reflectivity measurements provide a way to obtain the complex dielectric function, $\epsilon(0, \omega)$. Either ellipsometry or measurement of the reflectivity at normal incidence over a wide spectral range and subsequent Kramers–Kronig analysis of the data can be used. These methods are also not without their pitfalls. Reflectivity is extremely dependent on surface conditions, and features are easily obscured by scattering from imperfect surfaces or by adsorbed layers. The best measurements are therefore made on surfaces that have been freshly cleaved under the ultrahigh vacuum of the sample chamber or that have been carefully prepared by mechanical polishing and subsequent electropolishing, although the latter method can introduce surface impurities. Because of the extreme moisture and temperature sensitivity of the alkali metal anion salts that are the subject of this work, neither these techniques nor cleaning by ion bombardment could be used.

Kramers–Kronig analysis requires, in principle, knowledge of the frequency dependence of the reflectivity from zero to infinite frequencies. In many cases useful information can be obtained even if R is known only over a limited frequency range,

provided the data include the region below the threshold for direct optical transitions as well as most of the strong structure at higher energies. Extrapolation of the measured data to zero frequency is quite straightforward by calculating the reflectance from the dielectric constant which is normally easily obtainable. The extrapolation of R to higher frequencies on the other hand does not follow a simple rule. Techniques useful when working with semiconductors have been given by Philipp and Ehrenreich (17). In the present work, reflectivity data were obtained only for the energy range $0.5 \text{ eV} < \hbar\omega < 3.6 \text{ eV}$. This range is not extensive enough to justify a Kramers–Kronig treatment. Instead, we obtained optical information by combining these new reflectivity measurements with the new measurements of the absorption spectrum of vapor-deposited thin solid films. The transmittance data were obtained for the energy range $1.35 \text{ eV} < \hbar\omega < 3.0 \text{ eV}$, although the energy range was extended slightly by extrapolation to $1.00 \text{ eV} < \hbar\omega < 3.0 \text{ eV}$.

Experimental

Polycrystalline samples of $\text{Na}^+\text{C222} \cdot \text{Na}^-$ were synthesized as described previously (1, 2). Crystals were grown by programmed cooling of a solution of $\text{Na}^+\text{C222} \cdot \text{Na}^-$ in a 1:2 mixture of methylamine/ethylamine. After initial cycling of the temperature by $\pm 5^\circ$ slightly below the saturation temperature, the solution was cooled from -10 to -65°C at a rate of $1^\circ\text{C}/\text{hr}$. Crystals of ca. 1 mm in size are easily obtained in this way. Some of these crystals were transferred under purified helium in an inert atmosphere glove box (Vacuum Atmospheres Model DLX-001-S-G) into a 5-mm quartz optical cell and sealed off under high vacuum ($< 10^{-5}$ Torr). Examination of the crystals at a magnification of ca. $100\times$ revealed many small grooves on

the surface as well as regions of silvery material on the predominantly shiny golden-copper-colored surface. Thus, the area suitable for measurement is very small, so that a microscopic technique was necessary.

The reflectivity spectrometer was constructed with an Ealing–Beck microscope body. The design is similar to the apparatus of Welber (18) and Yakushi *et al.* (19). A 150-W tungsten–halogen lamp was focused onto the secondary focal plane of the 10X NA.17 achromatic objective. A 90° thin film dielectric mirror directed the beam down through the objective onto the sample. With a 1-mm iris at the lamp and another in front of the 90° mirror, the light spot was ca. $40 \mu\text{m}$ in diameter. The long working distance and small acceptance cone ($< 20^\circ$) of the objective resulted in approximately normal incidence. The reflected light was spectrally analyzed with a Bausch & Lomb high intensity monochromator ($f3.5$) at a resolution of 10 nm from 350 to 800 nm and (with a different grating) 40 nm from 800 to 2500 nm. A UV-enhanced Si-photodiode (UDT-UV 005) was used for the 350- to 800-nm range and a thermoelectrically cooled PbS element (IR Industries 2757) from 800 to 2500 nm. The latter detector is sensitive up to 3500 nm, but the combination of low lamp output and the characteristics of the dielectric mirror restrict the measurements to $\lambda < 2500$ nm. The light was mechanically chopped, and the signal from the photoelements, which was preamplified with home-built amplifiers integrated into the detector housing, was synchronously detected with a PAR Model 126 lock-in amplifier. A first-surface aluminum mirror was used as a reflectance standard with its reflectivity set to 100% over the whole experimental range.

The lamp and electronic components were stable enough that a precision of 1% was easily achieved. Stray light from reflections on the windows of the cell was effectively suppressed by use of suitable iris diaphragms in the microscope barrel and was

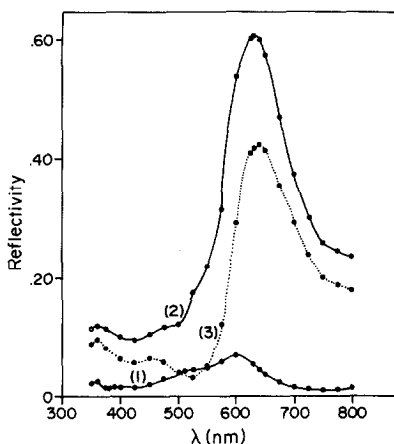


FIG. 1. Reflectivity (relative to a first-surface aluminum mirror) of three single crystals of $\text{Na}^+\text{C}_{222} \cdot \text{Na}^-$. The continuous curves in this and the other figures are drawn as an aid to the eye and do not represent calculated curves.

generally $<1\%$. The rough surface condition of the sample, and the lack of an x - y - z tilting stage to ensure exact normal incidence of the light beam on the crystal surface, limited the accuracy to $\sim 20\%$. Higher harmonics were suppressed by using appropriate filters (Corning 254, 2303, and 2424).

$\text{Na}^+\text{C}_{222} \cdot \text{Na}^-$ was synthesized in thin film form for transmittance measurements by the direct evaporation of sodium and cryptand in a vacuum evaporator. The materials were resistively heated at 10^{-5} Torr and the vapors were simultaneously deposited on a cooled quartz substrate suspended above the vapor sources, or were deposited in alternate layers of metal and complexant. The deposition rates were monitored with a VEECO thickness monitor, Series QM-300, Model 301. The deposition rates and times were used to determine the thickness of films. The blue (by transmission) films appeared to be smooth and uniform, and thick films gave the characteristic golden color of $\text{Na}^+\text{C}_{222} \cdot \text{Na}^-$ by reflectance. The microscopic uniformity of these films has not, however, been confirmed by *ex situ* electron microscopy.

An *in situ* spectrometer was constructed to measure the transmission spectrum of $\text{Na}^+\text{C}_{222} \cdot \text{Na}^-$ films. Light from a 100-W Aries quartz tungsten-halogen lamp in a universal lamp housing (Model 40-130) was focused onto the entrance slit of the monochromator after being chopped by an Optical Engineering attenuator. The chopping frequency was monitored by a photodiode detector that provided a signal for the lock-in amplifier. The light was monochromated by a Jarrell-Ash Model 82-000 series Ebert scanning monochromator with straight-edged slits that were variable between 0 and $2000 \mu\text{m}$. A Jarrell-Ash diffraction grating (Model 980-28-20-22) that had been blazed for 500 nm with 1180 grooves/mm was used with a Corning 744 filter. The light beam was directed into the vacuum system through a sapphire window and was reflected vertically through a focusing lens so that it passed through the film and substrate and reached the detector. A United Detector Technology photovoltaic photodiode detector (Model PIN-5DP) was used with a home-built preamplifier and was housed in an aluminum can in the vacuum space. The signal from the preamplifier was processed by a home-built lock-in amplifier and was recorded with a Linear X-Y recorder (Model 8036). The reference spectra were measured through bare substrates prior to the evaporation of sodium or cryptand.

Results

For purposes of illustration, the reflectivity of three different crystals in the "visible" region is shown in Fig. 1. Crystal 1 had obviously changed and appeared silver in color, while the other two crystals showed the golden color typical of $\text{Na}^+\text{C}_{222} \cdot \text{Na}^-$. Also, the peak reflectivity of crystal 1 was only 7%, whereas the other two crystals had maximum reflectivities of 61 and 43%, respectively. The wavelength of the reflectivity maximum for crystal 1 was blue-

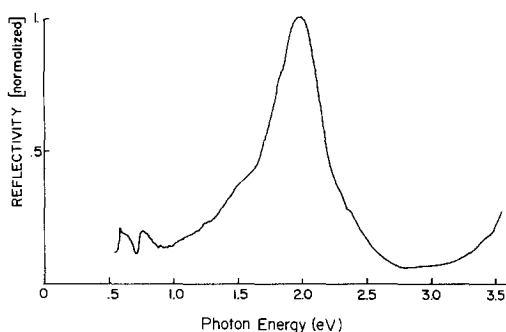


FIG. 2. Normalized reflectivity (composite spectra) as a function of the photon energy for single crystals of $\text{Na}^+\text{C222} \cdot \text{Na}^-$.

shifted and this peak had a pronounced shoulder at ~ 500 nm, which was absent in the other crystals. Since the processes that lead to this initial spectral change and ultimately to complete decomposition are unknown, only the spectra of fresh, intact crystals of $\text{Na}^+\text{C222} \cdot \text{Na}^-$ will be considered.

In Fig. 2 the complete normalized composite spectrum, obtained by combining data from several crystals, is shown on an energy scale. The peaks at 0.59 and 0.75 eV (4760 and 6130 cm^{-1}) are probably due to higher harmonics of C–H vibrations in the cryptand molecule. Apart from this structure, the reflectance shows only one broad peak at 1.97 ± 0.03 eV (630 nm) with a full-width at half-maximum of 0.51 eV. The increase in reflectivity above 3.0 eV suggests that there may be a second maximum at higher energies.

The absorption spectra of several thin films of $\text{Na}^+\text{C222} \cdot \text{Na}^-$ were measured. While most of the spectra had nearly identical lineshapes that were also similar to those found for films produced by solvent evaporation, a few films, deposited at low temperatures, had abnormally broad bands and high baselines, indicative of an inhomogeneous film that contained large amounts of unreacted metal and cryptand. The typical absorption shape gave a peak

maximum at 650 ± 10 nm (1.91 eV) with a full-width at half-maximum of 0.37 eV. The spectral bands also showed the typical asymmetry of the Na^- absorption, in which the high energy side of the peak has more absorption in the wings than the low energy side.

The absorption coefficient, α , as a function of wavelength was calculated for all the films measured. The areas under these curves were determined in order to estimate the oscillator strength of the transition. The oscillator strength, f , is defined by

$$f = 4.33 \times 10^{-9} C^{-1} \int k(\bar{\nu}) d\bar{\nu}, \quad (4)$$

in which C is the concentration of the absorbing species in moles per liter. In crystals of $\text{Na}^+\text{C222} \cdot \text{Na}^-$, C is 2.52 M. The value of f was approximately 2 for some films, but other films, particularly inhomogeneous films that contained large amounts of unreacted metal and cryptand, had values as low as 1.0. The oscillator strength is expected to be close to 2.0 based on its value for Na^- in solution (20). Because of this, the absorption coefficients of four films with very similar lineshapes were scaled to give an oscillator strength of 2.0. At the absorption maximum, this composite spectrum yielded an average value of the molar decadic absorption coefficient, $\alpha/\ln 10$, of $7.1 \pm 0.5 \times 10^4 M^{-1} \text{cm}^{-1}$, in comparison with the value for Na^- in solution of $8.2 \pm 0.3 \times 10^4 M^{-1} \text{cm}^{-1}$ (20). The index of absorption, k , was then calculated from the average values of α by using the relationship $\alpha = 4\pi k/\lambda$. The relationship between the spectral shape of vapor deposited films and films grown from solution can be seen in Fig. 3 in which the values of k from the composite vapor deposited film spectra are compared with those of solvent-evaporated films. It can be seen that the peak for the vapor-deposited film is substantially narrower than for the solvent-evaporated film and has a less-pronounced shoulder at 2.5

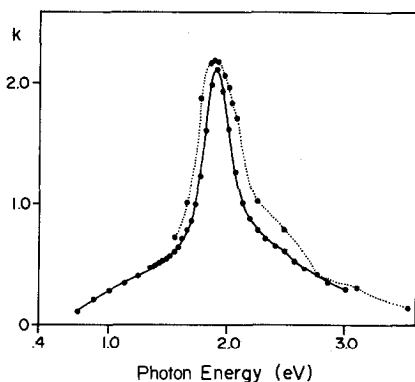


FIG. 3. The index of absorption, k , versus photon energy for films of $\text{Na}^+\text{C222} \cdot \text{Na}^-$ formed by solvent evaporation (dotted line) and by vapor deposition (solid line).

eV. We attribute this to better uniformity of the vapor deposited film.

These values of k were used with the value of R obtained from the composite reflectivity spectrum to calculate the index of refraction, n (Eq. (1)), as well as the complex dielectric constant from the relationships $\epsilon_1 = n^2 - k^2$ and $\epsilon_2 = 2nk$. The results are shown in Fig. 4. The energy loss function, $\text{Im}(\epsilon^{-1})$, calculated from

$$\text{Im}(\epsilon^{-1}) = \epsilon_2 / (\epsilon_1^2 + \epsilon_2^2) \quad (5)$$

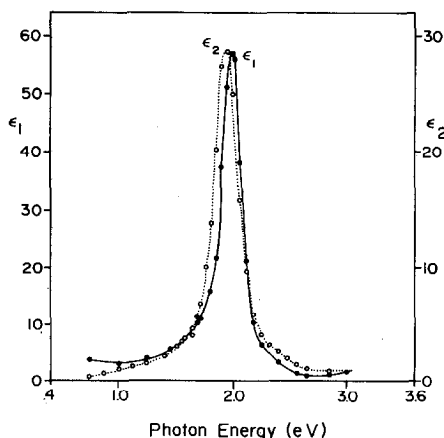


FIG. 4. The components of the complex dielectric constant of $\text{Na}^+\text{C222} \cdot \text{Na}^-$ as a function of the photon energy.

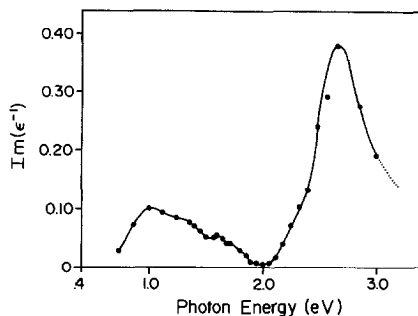


FIG. 5. The energy loss function, $\text{Im}(\epsilon^{-1})$, for $\text{Na}^+\text{C222} \cdot \text{Na}^-$ as a function of the photon energy.

is shown in Fig. 5. This function is expected to exhibit maxima where collective electron oscillations are excited (21–23). Within experimental error, only the peak centered at 2.6 eV (Fig. 5) might be significant. This energy coincides with the pronounced minimum in the reflectivity and the shoulder found in the optical absorption of thin films. The threshold for photoemission from the Na^- species is also found near this wavelength (13). The absolute value of the peak in $\text{Im}(\epsilon^{-1})$ is small, however, and the uncertainties in the absorbance and reflectivity data are large in this region. Thus, while we can be fairly confident that there is no significant peak between 0.6 and 2.0 eV, direct measurements of the energy loss function (in progress) will be required to verify the existence of a peak at high energies.

Another problem in combining reflectance and transmittance data is the fact that, as shown in Fig. 6, the peak in k occurs at slightly lower energies than that in n , contrary to theory for a single transition (24). Since sodide crystals are strongly anisotropic, different faces might have different reflectivity spectra so that the maximum in reflectivity could appear at higher energies than the maximum in the absorption spectrum. The latter averages over all possible orientations of the polycrystalline films.

The real part of the dielectric constant, ϵ_1 , reaches a value of 3 ± 1 at the lowest

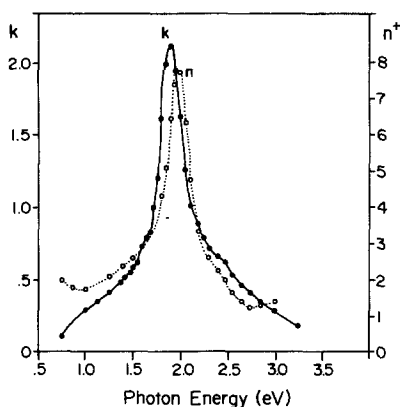


FIG. 6. The index of refraction, n (dotted line), and the index of absorption, k (solid line), of $\text{Na}^+\text{C222} \cdot \text{Na}^-$ as a function of photon energy.

frequencies. Direct measurements of the dielectric constant in the frequency range 0.1–10 MHz yield $\epsilon = 2.4 \pm 0.4$, nearly independent of frequency and temperature (15). The latter value of ϵ and the Clausius–Mosotti equation

$$P_M = \frac{M(\epsilon - 1)}{\rho(\epsilon + 2)} \quad (6)$$

yield a molar polarization, P_M , of $140 \pm 20 \text{ cm}^3 \text{ mol}^{-1}$. To estimate the molar polarization of the cryptand molecule, we use the fact that atom, bond and group polarizations are additive. The values compiled by Vogel *et al.* (25) yield a calculated molar polarization of $108 \pm 5 \text{ cm}^3 \text{ mol}^{-1}$ for C222, while the Na^+ cation adds the negligible contribution $0.5 \text{ cm}^3 \text{ mol}^{-1}$. To obtain P_M for the sodide ion, we use the equation

$$P_M = -2.64 + 2.01 \times 10^{24}(r)^3 \quad (7)$$

in which r is the anionic radius. Equation (7) gives an excellent fit (correlation coefficient 0.9989) to the experimental molar polarizations of F^- , Cl^- , Br^- , and I^- , which are 2.5, 9.0, 12.5, and $19.0 \text{ cm}^3 \text{ mol}^{-1}$, respectively (24), and agrees with the prediction from electrostatic considerations that the polarizability of a conducting sphere is equal to its volume. By extrapolating Eq.

(7) to the experimental radius of Na^- as obtained from structural data, 2.6 \AA (2), we obtain a value of $33 \pm 4 \text{ cm}^3 \text{ mol}^{-1}$ for the molar polarization of the sodide ion. The total calculated molar polarization of $\text{Na}^+\text{C222} \cdot \text{Na}^-$ is thus $142 \pm 6 \text{ cm}^3 \text{ mol}^{-1}$, in excellent agreement with experimental values.

Conclusions

Although quantitative measurements of the optical properties of alkaldes are difficult because of their extreme reactivity and tendency to decompose thermally, these data provide a consistent picture of the nature of the sodide salt $\text{Na}^+\text{C222} \cdot \text{Na}^-$. At low energies the optical reflectivities and absorption coefficients are compatible with the low-frequency dielectric constant data. The low-energy refractive index is also in agreement with the value expected for the cryptated cation and the highly polarizable anion Na^- .

Consideration of the structure (2), Na NMR spectrum (10–12) and optical properties of $\text{Na}^+\text{C222} \cdot \text{Na}^-$ shows conclusively that Na^- is a “genuine” alkali metal anion with two electrons in the $3s$ orbital and that the ground state is not strongly perturbed from that in the gaseous state. The intense optical absorption band described in this paper is assigned to a $3s^2 \rightarrow 3s3p$ transition with an oscillator strength of ~ 2.0 . Thus, we expect no strong absorption bands of Na^- at higher frequencies due to excitation of the $3s$ electrons. The shoulder in the absorption spectrum at $\sim 2.5 \text{ eV}$ may be due to a transition to the conduction band since conductivity measurements show a bandgap of this magnitude (15).

The ability to measure the reflectance spectrum of small reactive crystals will be of particular importance to the study of electrides, salts in which the anions are all trapped electrons (4, 26–28). Qualitative transmission spectra indicate that the elec-

trons range from a localized state in the case of $\text{Cs}^+(18\text{C}6)_2 \cdot e^-$ (26, 27) to delocalized in $\text{K}^+\text{C}222 \cdot e^-$ (4). The former shows a well-defined absorption peak in the near infrared at 0.8 eV, while the latter has an apparent plasma edge at about 1.4 eV. Because thin films can have a variety of imperfections, it is important to complement optical transmission studies with reflectance measurements. Such studies of both alkali-ides and electrides are in progress.

Acknowledgments

This research was supported by the National Science Foundation—Solid State Chemistry Grants DMR 79-21979 and DMR 84-03494. We are grateful to Professor Stuart Solin of the Department of Physics and Astronomy, Michigan State University, for helpful discussions of optical properties.

References

1. J. L. DYE, J. M. CERASO, M. T. LOK, B. L. BARNETT, AND F. J. TEHAN, *J. Amer. Chem. Soc.*, **96**, 608 (1974).
2. F. J. TEHAN, B. L. BARNETT, AND J. L. DYE, *J. Amer. Chem. Soc.* **96**, 7203 (1974).
3. B. VAN ECK, L. D. LE, D. ISSA, AND J. L. DYE, *Inorg. Chem.* **21**, 1966 (1982).
4. J. L. DYE, *Prog. Inorg. Chem.* **32**, 327 (1984).
5. J. L. DYE, *J. Phys. Chem.* **88**, 3842 (1984).
6. J. L. DYE, M. R. YEMEN, M. G. DAGUE, AND J.-M. LEHN, *J. Chem. Phys.* **68**, 1665 (1978).
7. M. G. DAGUE, J. S. LANDERS, H. L. LEWIS, AND J. L. DYE, *Chem. Phys. Lett.* **66**, 169 (1979).
8. J. L. DYE, M. G. DAGUE, M. R. YEMEN, J. S. LANDERS, AND H. L. LEWIS, *J. Phys. Chem.* **84**, 1096 (1980).
9. A. SCHINDEWOLF, L. D. LE, AND J. L. DYE, *J. Phys. Chem.* **86**, 2284 (1982).
10. J. L. DYE, C. W. ANDREWS, AND J. M. CERASO, *J. Phys. Chem.* **79**, 3076 (1975).
11. A. ELLABOUDY, M. L. TINKHAM, B. VAN ECK, J. L. DYE, AND P. B. SMITH, *J. Phys. Chem.* **88**, 3852 (1984).
12. A. ELLABOUDY AND J. L. DYE, *J. Magn. Reson.* **66**, 491 (1986).
13. S. JAENICKE AND J. L. DYE, *J. Solid State Chem.* **54**, 320 (1984).
14. J. L. DYE, *Angew. Chem. Int. Ed. Engl.* **18**, 587 (1979).
15. J. PAPAIOANNOU, S. JAENICKE, AND J. L. DYE, *J. Solid State Chem.* **67**, 122-130 (1987).
16. L. D. LE, D. ISSA, B. VAN ECK, AND J. L. DYE, *J. Phys. Chem.* **86**, 7 (1982).
17. H. R. PHILIPP AND H. EHRENREICH, in "Semiconductors and Semimetals" (R. K. Willardson and A. C. Beer, Eds.), Vol. 3, p. 93. Academic Press, New York (1967).
18. B. WELBER, *Rev. Sci. Instrum.* **47**, 183 (1974).
19. K. YAKUSHI, H. KURODA, R. HOLLMAN, AND W. A. LITTLE, *Rev. Sci. Instrum.* **53**, 1292 (1982).
20. M. G. DEBACKER AND J. L. DYE, *J. Phys. Chem.* **75**, 3092 (1971).
21. P. NOZIERES AND D. PINES, *Phys. Rev.* **113**, 1254 (1959).
22. H. EHRENREICH AND H. R. PHILIPP, *Phys. Rev.* **128**, 1622 (1962).
23. H. R. PHILIPP AND H. EHRENREICH, *Phys. Rev.* **129**, 1550 (1963).
24. J. M. ZIMAN, in "Principles of the Theory of Solids," p. 227, Cambridge Univ. Press, London (1964).
25. A. I. VOGEL, W. T. CRESSWELL, G. H. JEFFREY, AND J. LEICESTER, *J. Chem. Soc.*, p. 514 (1952).
26. A. ELLABOUDY, J. L. DYE, AND P. B. SMITH, *J. Amer. Chem. Soc.* **105**, 6490 (1983).
27. J. L. DYE AND A. ELLABOUDY, *Chem. Brit.* **20**, 210 (1984).
28. S. B. DAWES, D. L. WARD, R. H. HUANG, AND J. L. DYE, *J. Amer. Chem. Soc.* **108**, 3534 (1986).